

Affordable echelle spectroscopy of the eccentric HAT-P-2, WASP-14, and XO-3 planetary systems with a sub-meter-class telescope

Z. Garai^{1,2}, T. Pribulla¹, L. Hambálek¹, E. Kundra¹, M. Vaňko¹, S. Raetz^{3,4}, M. Seeliger³, C. Marka⁵, and H. Gilbert³
 (1Astronomical Institute of SAS, Tatranská Lomnica, Slovakia; 2Slovak Central Observatory, Hurbanovo, Slovakia; 3Friedrich Schiller University, Jena, Germany; 4European Space Agency, Noordwijk, The Netherlands; 5Institute for Millimetric Radioastronomy, Granada, Spain)

Abstract

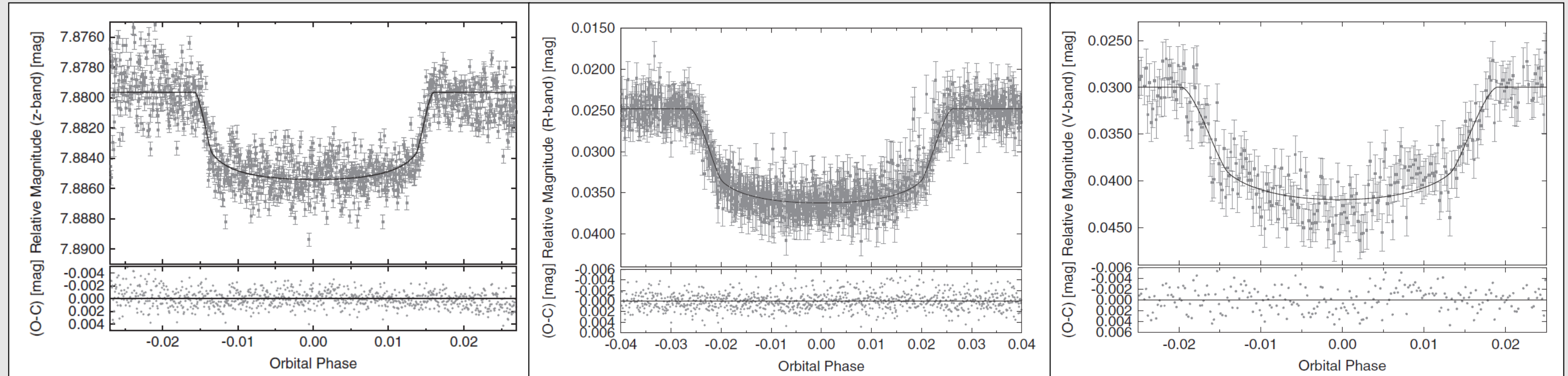
A new off-the-shelf, low-cost echelle spectrograph eShel was installed recently on the 0.6m telescope at the Stará Lesná Observatory (SLO) – G1 (Slovakia). We describe the radial velocity (RV) analysis of the first three transiting planetary systems, namely HAT-P-2, WASP-14, and XO-3, observed with this instrument. First, we reduced and analyzed our RV observations. Subsequently, we compared our data with previously published RV data. We were curious about the precision of our measurements in comparison to that of the RV data achieved with echelle spectrographs of other sub-meter-, meter- and 2-m-class telescopes. Another question was the applicability of our RV data for modeling orbital parameters. For this purpose, the previously published data were analyzed in the same way as our RV data in order to determine and compare the parameters. Finally, we combined and analyzed all used RV data per object.

Properties of the instrumentation at SLO-G1



The RV observations were performed at SLO-G1 with a 0.6m, f/12.5 Zeiss Cassegrain telescope (see figure left). The fiber injection and guiding unit (hereafter FIGU) of the eShel spectrograph is mounted in the Cassegrain focus of the telescope. The FIGU is connected to the calibration unit (ThAr hollow cathode lamp, tungsten lamp, blue LED) in the control room (see figure upper right) and to the echelle spectrograph itself in the cellar below the dome (see figure lower right). The collimated beam is dispersed by a high-efficiency R2 echelle grating with 79 grooves/mm. The maximum resolution of the eShel spectrograph reaches $R \sim 12\,000$ (Pribulla et al. 2015).

An overview of the selected planetary systems; observations and data analysis

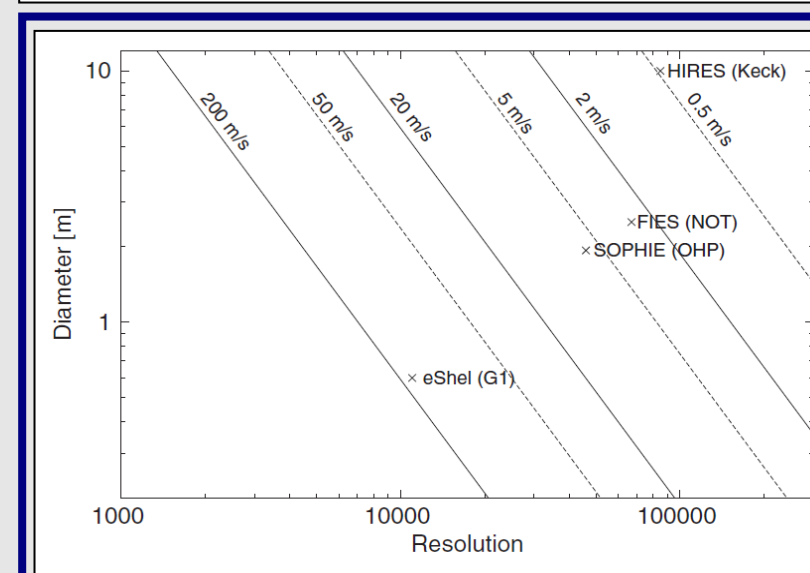
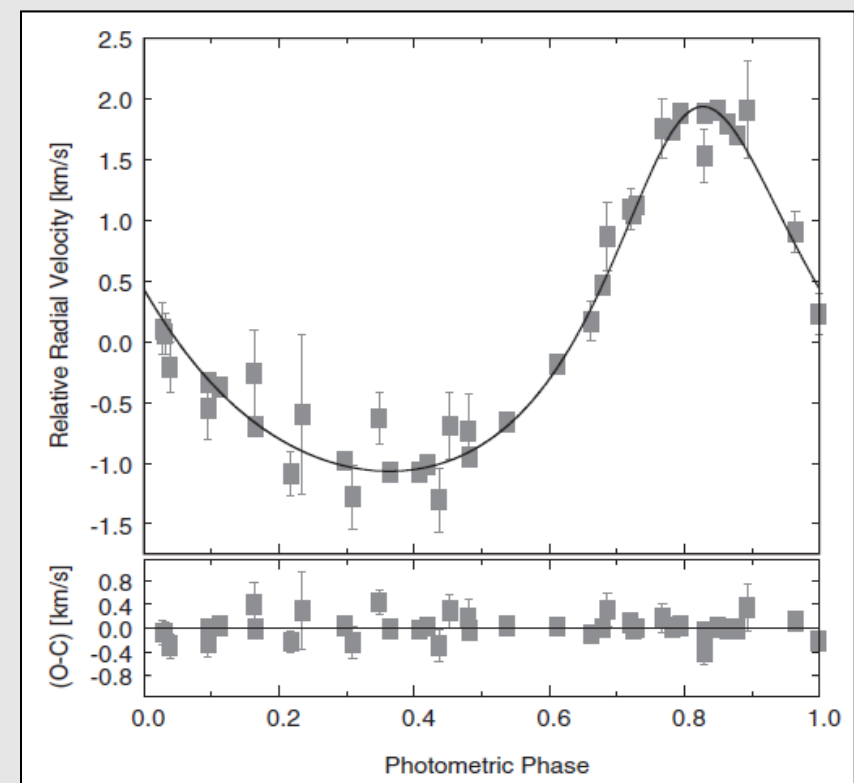
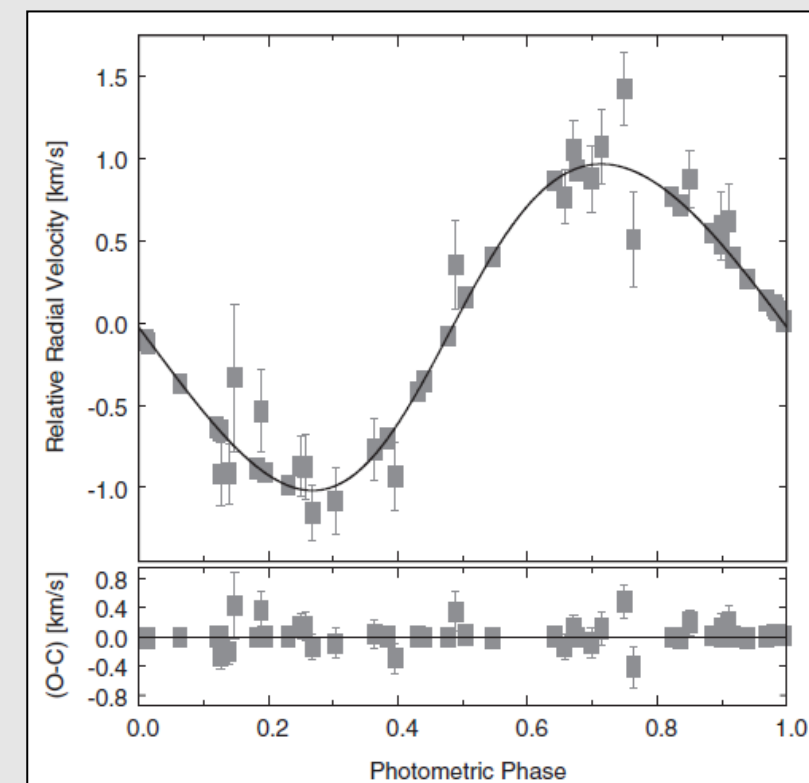
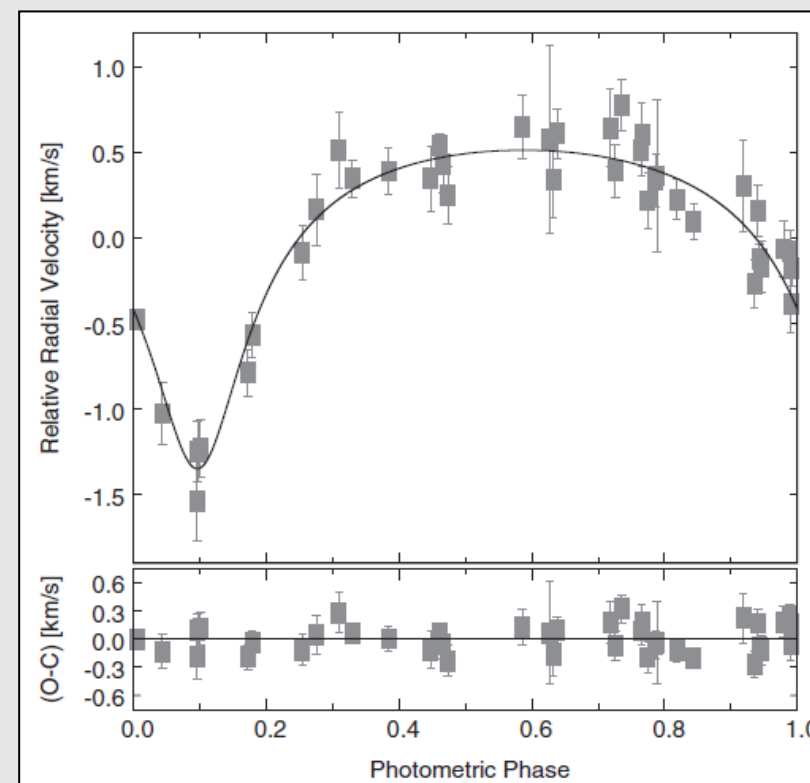


The objects were selected according to the RV amplitude, brightness, and the sky position. All three systems are, however, very interesting because they are characterized by close-in, but apparently eccentric orbits, and therefore represent potentially important systems to constrain the migration as well as tidal and thermal evolution of gas giant planets (Bakos et al., 2007; Johns-Krull et al., 2008; Joshi et al., 2009). Using our instrumentation, we obtained 20 RV measurements per planetary system. The data were reduced using IRAF package tasks, Linux shell scripts, and FORTRAN programs as described in Pribulla et al. (2015). We then used the code JKTEBOP (Southworth, Maxted, & Smalley, 2004). This code can fit RVs simultaneously with a light curve; hence the orbital parameters of the three transiting planets were calculated from the RV data, together with the photometric data. The used transit light curve of HAT-P-2b, WASP-14b, and XO-3b is depicted on left panel (taken from the HATNet archive), middle panel (taken from Raetz et al. 2015), and right panel (observed at the Teide Observatory), respectively. We fitted RV data from different sources simultaneously with exactly the same photometric data per object. First, we fitted only our G1 RV data simultaneously with the photometric data. Subsequently, we fitted previously published RV data from other sub-meter-, meter-, and 2-m-class telescopes, simultaneously with the photometric data, in the same way as we described above, in order to compare the results. In the case of HAT-P-2, we used the RV data published by Csák et al. (2014). Observations were carried out at the Gothard Astrophysical Observatory (GAO; a 0.5m telescope), Szombathely, and at the Piskéštető Mountain Station (PO; a 1m telescope) with the same eShel spectrograph. For WASP-14, we adopted the RV data published by Joshi et al. (2009), which were collected with the FIES instrument in medium-resolution mode (Telting et al., 2014), mounted on the 2.5m Nordic Optical Telescope (NOT) and with the SOPHIE spectrograph in high-efficiency mode (Perruchot et al., 2008) on the 1.93m telescope at the Haute-Provence Observatory (OHP). In the case of XO-3, we used the RV data published by Hébrard et al. (2008), which were collected with the SOPHIE in high-resolution mode. Finally, we combined and analyzed all used data per object.

Results: the best fit parameters and spectroscopic models

Parameter	Value from Lit.	Lit. Ref.	Value from G1	Value from GAO + PO	Value from G1 + GAO + PO
HAT-P-2b					
Zero transit time T_0 (HJD - 2 400 000)	54387.4937(7)	[P10]	54387.4937	54387.4937	54387.4937
Orbital period P_{orb} (days)	5.633472(6)	[P10]	5.633472	5.633472	5.633472
Normalized semi-major axis a/R_p	8.9(3)	[P10]	—	—	—
Sum of fractional radii $(R_p + R_p)/a$	—	—	0.143(11)	0.130(6)	0.119(5)
Ratio of the radii R_p/R_s	0.0722(6)	[P10]	0.0677(2)	0.0678(2)	0.0678(2)
Inclination i (°)	86.7(8)	[P10]	86.4(4)	86.8(3)	87.2(3)
Eccentricity e	0.50910(48)	[L13]	0.58(4)	0.56(2)	0.510(16)
Periastron longitude ω (°)	188.09(39)	[L13]	165(6)	175(5)	181(5)
Systemic velocity γ (m/s)	-278(20)	[B07]	-279(44)	-197(31)	-220(22)
RV semi-amplitude K (m/s)	983(17)	[P10]	1,131(179)	904(52)	930(42)
Linear LD coefficient (z-band)	0.186	[C11]	0.186	0.186	0.186
Nonlinear LD coefficient (z-band)	0.302	[C11]	0.302	0.302	0.302
Light scale factor L_{sc} (mag)	—	—	7.87965(2)	7.87965(2)	7.87965(2)
Parameter	Value from Lit.	Lit. Ref.	Value from G1	Value from NOT + OHP	Value from G1 + NOT + OHP
WASP-14b					
Zero transit time T_0 (HJD - 2 400 000)	54463.5758(5)	[J09]	54463.5758	54463.5758	54463.5758
Orbital period P_{orb} (days)	2.243752(10)	[J09]	2.2437671(5)	2.2437669(2)	2.2437669(2)
Orbital semimajor axis a (AU)	0.0360(10)	[J09]	—	—	—
Stellar radius R_s (R_\odot)	1.30(6)	[J09]	—	—	—
Transit depth $(R_p/R_s)^2$ (mag)	0.0102(2)	[J09]	—	—	—
Sum of fractional radii $(R_p + R_p)/a$	—	—	0.180(12)	0.171(6)	0.171(6)
Ratio of the radii R_p/R_s	—	—	0.0973(8)	0.0972(8)	0.0972(8)
Inclination i (°)	84.3(6)	[J09]	85.1(8)	85.6(5)	85.6(5)
$k = e \cos \omega$	-0.02474(78)	[W15]	-0.02(3)	-0.0254(9)	-0.0253(9)
$h = e \sin \omega$	-0.0792(31)	[W15]	-0.03(6)	-0.085(2)	-0.085(2)
Systemic velocity γ (m/s)	-4,985(3)	[H11]	-4,985(48)	-4,985.0(1.7)	-4,985.0(1.7)
RV semi-amplitude K (m/s)	991(3)	[H11]	1,041(54)	993(3)	993(3)
Linear LD coefficient (R-band)	0.267	[C11]	0.267	0.267	0.267
Nonlinear LD coefficient (R-band)	0.324	[C11]	0.324	0.324	0.324
Light scale factor L_{sc} (mag)	—	—	-0.00521(8)	-0.00521(8)	-0.00521(7)
Parameter	Value from Lit.	Lit. Ref.	Value from G1	Value from OHP	Value from G1 + OHP
XO-3b					
Zero transit time T_0 (HJD - 2 400 000)	54449.8681(2)	[W08]	54449.8681	54449.8681	54449.8681
Orbital period P_{orb} (days)	3.191523(6)	[W08]	3.191523	3.191523	3.191523
Normalized semimajor axis a/R_s	7.0(3)	[W08]	—	—	—
Sum of fractional radii $(R_p + R_p)/a$	—	—	0.159(13)	0.143(9)	0.144(8)
Ratio of the radii R_p/R_s	0.0905(5)	[W08]	0.1012(19)	0.1005(19)	0.1005(19)
Inclination i (°)	84.2(5)	[W08]	84.0(9)	85.1(7)	85.1(7)
Eccentricity e	0.2769(17)	[W14]	0.255(19)	0.285(3)	0.285(3)
Periastron longitude ω (°)	346.3(1.3)	[W09]	346(13)	348.8(1.5)	348.9(1.5)
Systemic velocity γ (m/s)	-12,045(8)	[W09]	-12,045(51)	-12,030(7)	-12,030(7)
RV semi-amplitude K (m/s)	1,503(10)	[H08]	1,441(89)	1,502(10)	1,501(10)
Linear LD coefficient (V-band)	0.351	[C11]	0.351	0.351	0.351
Nonlinear LD coefficient (V-band)	0.311	[C11]	0.311	0.311	0.311
Light scale factor L_{sc} (mag)	—	—	-0.0001(2)	-0.0001(2)	-0.0001(2)

Fixed parameters are listed without errors. Parameters from Bakos et al. (2007) [B07], Pál et al. (2010) [P10], Lewis et al. (2013) [L13], Joshi et al. (2009) [J09], Hestroff et al. (2011) [H11], Wong et al. (2015) [W15], Winn et al. (2008) [W08], Winn et al. (2009) [W09], Hébrard et al. (2008) [H08], Wong et al. (2014) [W14], and Claret and Bloemen (2011) [C11] are summarized in the second column.



In the case of **HAT-P-2** we worked with 39 (20 + 19) RV measurements (upper left panel). The resulting G1 RVs show an average scatter of about 170 m/s. First, we fitted only our G1 RV data simultaneously with the photometric data. The best fit parameters are summarized in the table (left panel). Subsequently, we fitted GAO and PO RV data simultaneously with the photometric data. The average RV scatter of these data is about 177 m/s, comparable with our G1 RV scatter. Finally, we simultaneously fitted photometric and all RV data. The best fit parameters are also summarized in the table. The table shows that the parameter values derived from the G1 RV data are, in general, consistent with the values adopted from the literature. On the other hand, the values of the orbit eccentricity are more inconsistent, and we did not confirm the periastron longitude and the ratio of the radii. By comparing the G1 and GAO/PO RV data, we can state that parameter values are determined similarly.

In the case of **WASP-14** we worked with 47 (20+27) RV measurements (upper middle panel). Our RVs show an average scatter of about 220 m/s. First, we fitted only our G1 RV data, simultaneously with the photometric data. The best fit parameters are summarized in the table. In the next step, we fitted NOT and OHP RV data, simultaneously with the photometric data. In this case, the average RV scatter is only about 10 m/s. Finally, we simultaneously fitted the photometric and all RV data. The best fit parameters are also summarized in the table. The resulting parameter values are very similar, for example, in the case of the systemic velocity. The parameter h is more inconsistent. The value of the RV semi-amplitude K derived from G1 RVs, is far from the parameter K , derived from NOT/OHP RVs, however, if we consider 1σ error limits, these values are also in agreement. The situation is very similar if we compare the best fit parameter values derived from G1 RV data and the literature parameter values. Furthermore, we can also easily see that the parameter values derived from G1 RVs are, in general, more uncertain.

In the case of **XO-3** we worked with 39 (20+19) RV measurements (upper right panel). The average scatter of G1 RVs is about 260 m/s. First, we fitted only our G1 RV data, simultaneously with the photometric data. The best fit parameters are summarized in the table. Subsequently, we fitted OHP RV data, simultaneously with the photometric data. The average RV scatter of OHP data is about 35 m/s. As the final step, we simultaneously fitted photometric and all RV data. The best fit parameters are also summarized in the table. We can compare, for example, the periastron longitude, the systemic velocity, or the orbit eccentricity. The parameter values derived from our G1 RVs are, however, more uncertain. The best fit parameters resulting from G1 RVs are also, in general, consistent with the literature values, however, we can see, again, that the literature values are given with better accuracy. We did not confirm only the ratio of the radii.

Expected RV precision as a function of the telescope diameter and the spectrograph resolution is depicted in the figure in this panel. The precision is scaled to match the precision achieved for HAT-P-2 with eShel on the 0.6m telescope at Stará Lesná Obs. The precision curves assume the same exposure time, telescope-spectrograph throughput, and the same object. The expected precision reasonably matches the observed uncertainty.

Conclusions

- Based on our results, we can conclude that the spectrograph is a useful instrument for the study of objects with a relatively small RV amplitude. We achieved an average precision of about 170 m/s in the case of HAT-P-2, 220 m/s in the case of WASP-14, and 260 m/s in the case of the XO-3 system. These values are sufficient for exoplanet RV detections and spectroscopic follow-up measurements of massive exoplanets on close-in orbits. The accuracy is well comparable with the average RV scatter achieved with other sub-meter and meter-class telescopes. In comparison with 2-m-class telescopes, our instrumentation gives an RV scatter of about one order greater. This difference is primarily due to the telescope diameter size.
- On the other hand, our best fit results show that RV data obtained with our instrumentation can be used to determine orbital parameters of massive close-in exoplanets. In general, we can conclude that the best fit parameters resulting from the G1 RV data are in good agreement with the published parameters. Literature parameter values are, however, given with better accuracy.
- Furthermore, in comparison with NOT/OHP RV data, due to the relatively lower RV accuracy of G1 RV data, we can determine the system parameters with larger error interval only. This is also the reason why parameters derived from NOT/OHP RV data and from combined G1 and NOT/OHP observations are very similar (see the table). Since data obtained at G1 have lower accuracy, these are low-weighted during the model-fitting procedure when we combined G1 and NOT/OHP observations, and have minimal influence on parameter determination.
- Recently, we published our results in the journal *Astronomical Notes* (Garai et al.: 2017, AN 338, 35). For other details see the published paper at the web-page <http://adsabs.harvard.edu/abs/2017AN...338...35G>.

Acknowledgements

The authors thank V. Kollár for technical assistance, B. Csák for the RV data, and J. Budaj for comments and discussion. This work was supported by the VEGA grant of the Slovak Academy of Sciences (No. 2/0143/14), the Slovak Research and Development Agency (Contract No. APVV-0158-11), the Slovak Central Observatory Hurbanovo, and the realization of the Project ITMS (No. 26220120029), based on the Supporting Operational Research and Development Program financed from the European Regional Development Fund. M.S. thanks piezosystem Jena, for financial support.

References

- Bakos, G.A., Kovács, G., Torres, G., et al. 2007, *ApJ*, 670, 826
- Csák, B., Kovács, J., Szabó, Gy.M., Kiss, L.L., Dózsa, Á., Sódor, Á., & Jankovics, I. 2014, *CoSka*, 43, 183
- Hébrard, G., Bouchy, F., Pont, F., et al. 2008, *A&A*, 488, 763
- Johns-Krull, Ch.M., McCullough, P.R., Burke, Ch.J., et al. 2008, *ApJ*, 677, 657
- Joshi, Y.C., Pollacco, D., Collier Cameron, A., et al. 2009, *MNRAS*, 392, 1532
- Perruchot, S., Kohler, D., Bouchy, F., et al. 2008, *SPIE*, 7014, 12
- Pribulla, T., Garai, Z., Hambálek, L., et al. 2015, *AN*, 336, 682
- Raetz, S., Maciejewski, G., Seeliger, M., et al. 2015, *MNRAS*, 451, 4139
- Southworth, J., Maxted, P.F.L., & Smalley, B. 2004, *MNRAS*, 351, 1277
- Telting, J.H., Avila, G., Buchhave, L., et al. 2014, *AN*, 335, 41